

## Ductile Fracture Prediction of 316LN Stainless Steel in Hot Deformation Process

Jian-li HE<sup>1,2</sup>, Juan LIU<sup>2</sup>, Zhen-shan CUI<sup>2</sup>, Chao-zhong YANG<sup>2</sup>, Fei CHEN<sup>2</sup>

(1. School of Materials Engineering, Shanghai University of Engineering Science, Shanghai 201620, China;

2. National Engineering Research Center for Die and Mold CAD, School of Materials Science and Engineering, Shanghai Jiao Tong University, Shanghai 200030, China)

**Abstract:** A ductile fracture criterion of 316LN stainless steel, combined with the plastic deformation capacity of material and the stress state dependent damages, was proposed to predict ductile fracture during hot deformation. To the end, tensile tests at high temperatures were first performed to investigate the fracture behavior of 316LN stainless steel. The experimental results show the variation of the critical fracture strain as a function of temperature and strain rate. Second, the criterion was calibrated by using the upsetting tests and the corresponding numerical simulations. Finally, the proposed fracture criterion was validated by the designed tests and the corresponding finite element (FE) simulation. The results show that the criterion can successfully predict the onset of ductile fracture at elevated temperatures.

**Key words:** ductile fracture criterion; FE simulation; upsetting test; fracture behavior; 316LN stainless steel

316LN stainless steel has the characteristics of excellent high temperature strength, high corrosion resistance and toughness, which make it be widely applied as key parts of nuclear power equipment such as the primary piping, the intermediate heat exchanger and the prototype fast breeder reactor (PFBR)<sup>[1,2]</sup>. However, 316LN stainless steel consists of the single-phase austenite, which results in no phase transformation during heat treatments. So, it is necessary to obtain fine and uniform grain structure by forging<sup>[3]</sup> in order to meet high quality requirements. The forging process usually has the characteristics of the distribution of non-uniform temperature, multi-step deformation, narrow forging temperature range and high resistance to deformation<sup>[4]</sup>, which is easy to result in the internal or surface cracking. So, how to predict cracking in the forming process is of vital importance.

Over the years, the remarkable results of predicting cracks by ductile fracture criteria in cold or hot forming processes were achieved, and a large amount of liter-

atures on ductile fracture criteria were available<sup>[5-12]</sup>. Johnson and Cook<sup>[11]</sup> developed a criterion during hot forming, in which an accumulating damage parameter was defined as a function of the weighted integral with respect to the current effective strain and the reciprocal of the effective fracture strain. Some researchers<sup>[9-12]</sup> used Johnson and Cook's criterion to predict the material fracture behavior of the structural steel and aluminium alloy and the results indicated that this criterion is limited under some conditions. Alexandrov et al.<sup>[13]</sup> established a criterion of aluminium alloy during hot forming and the predicted result was in good agreement with experimental one. However, the complexity of the forging process of large equipments makes it difficult to predict the formation of forging cracks by using existing ductile criteria. So, in this paper, a ductile criterion of 316LN stainless steel was proposed to predict the occurrence of cracks during hot deformation. The fracture behavior of 316LN stainless steel was first investigated based on

---

**Foundation Item:** Item Sponsored by National Science and Technology Major Project of China (2011ZX04014-051); National Basic Research Program of China (2011CB012903); 085 Project of Shanghai University of Engineering Science of China (nhky-2013-05)

**Biography:** Jian-li HE, Doctor; **E-mail:** hejianling792@163.com; **Received Date:** August 25, 2013

**Corresponding Author:** Zhen-shan CUI, Doctor; Professor; **E-mail:** cuiz@sjtu.edu.cn

the tensile tests at various temperatures and strain rates. Experimental results indicated that the critical fracture strain depends on temperature and strain rate, based on which a critical fracture strain model was established. Then, the parameters in the proposed criterion were defined by different tests and the numerical simulations. To verify the accuracy of the proposed criterion, finally, the designed tests and the corresponding finite element (FE) simulations with the implanted criterion were conducted.

## 1 Experiments

The chemical composition of 316LN stainless steel is given in Table 1. The tensile specimens shown in Fig. 1 were machined. The tensile tests were performed under a Gleeble-3500 thermo-mechanical simulator at various temperatures (1123–1473 K) and strain rates (0.001–1.000 s<sup>-1</sup>). Before the tensile tests, the specimens were heated to the predetermined temperature at a heating rate of 283 K/s and

**Table 1 Chemical composition of 316LN forging ingot**

													mass%	
C	Si	Mn	Cr	Mo	Ni	Cu	S	P	Co	Sb	N	Pb	As	Sn
0.02	0.22	1.68	17.66	2.51	11.94	0.06	0.003	0.005	0.03	0.0016	0.148	0.002	0.004	0.005

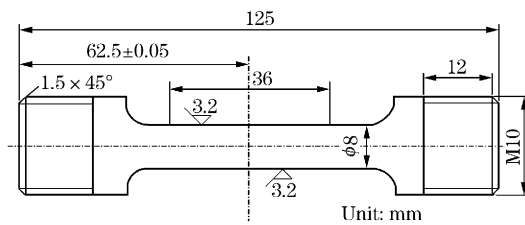


**Fig. 1 Dimensions of the tensile specimen**

held for 3 min.

## 2 Experimental Results

The true stress-true strain curves, as illustrated in Fig. 2, represent the combined effects of strain, strain rate, and deformation temperature. It can be seen from Fig. 2 that the flow stress is sensitive to the temperature and strain rate. Both the peak stress

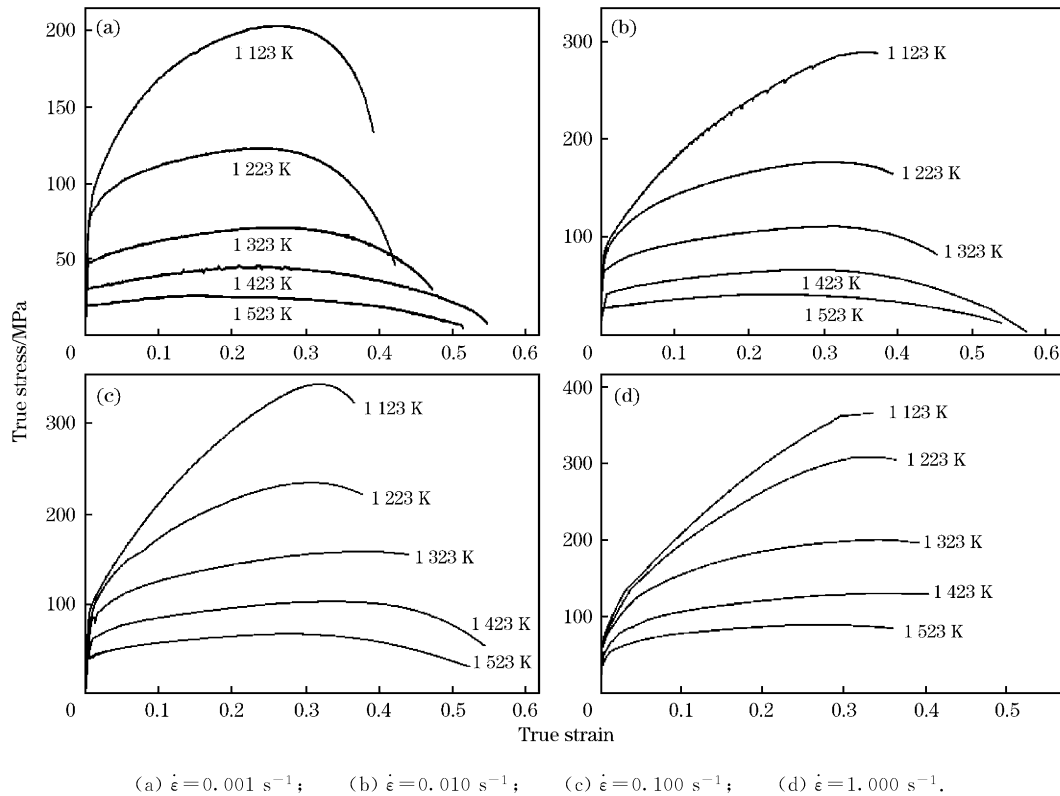


**Fig. 2 Relationships between true stress and true strain for 316LN at different strain rates**

$\sigma_p$  and peak strain  $\epsilon_p$  decrease in a similar manner with rising temperature  $T$  and declining strain rate

$\dot{\epsilon}$ , for which the declining dislocation density and large dynamic recrystallization (DRX) grain size mi-

croscopically appear. This is because that nucleation is retarded by increasingly fast concurrent straining which introduces additional dislocations into the forming nucleus.

In tensile tests, engineering materials during hot deformation can sustain large deformation after necking. This property can be advantageous to the manufacturing process and mechanical performance. However, it causes difficulties in critical strain measurement, particularly at lower strain rates and high temperatures. The critical fracture strain  $\epsilon_f$ , which is the strain when the necking occurs, is an important parameter of ductile fracture model and can reflect the plastic deformation capacity. Here, using a measurement method<sup>[14]</sup>, in which the zone with non-uniform deformation after necking is converted to be an equivalent zone with uniform deformation according to the constancy of volume, the critical fracture strains were obtained at various temperatures and strain rates, as shown in Fig. 3.

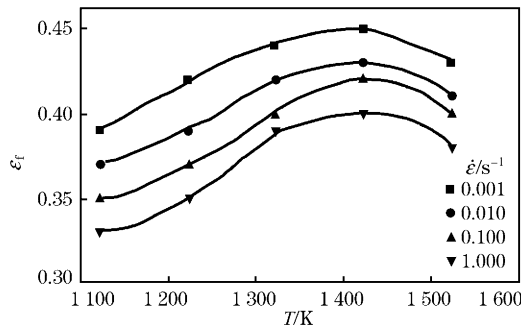


Fig. 3 Values of critical fracture strain at various strain rates and temperatures

### 3 Critical Fracture Strain Model

It can be seen from Fig. 3 that the values of  $\epsilon_f$  vary clearly with temperatures and strain rates. At a constant strain rate,  $\epsilon_f$  increases gradually to the peak value and then drops with increasing temperature. This is because the capabilities of the dynamic recovery and dynamic recrystallization become strong when the temperature increases. The dislocation density decreases and the probability of micro-cracks initiation increases as the dislocation pile-up descends. Once the temperature exceeds some certain limit, the grain boundary turns weak and the micro-cracks may be easy to occur at the grain boundary. The temperature corresponding to the peak value of  $\epsilon_f$  is called critical temperature hereby. However, the effect of strain rate on  $\epsilon_f$  is different from the effect of temperature. At a constant temperature,  $\epsilon_f$  de-

creases with increasing the strain rate. This is because there is no enough time for the softening or dislocation annihilation at high strain rate while the thermal activation energy decreases, which eventually leads to an increase in micro-cracks. In view of the effects of temperature and strain rate on ductile fracture, it is assumed that the critical fracture strain during hot forming can be fitted into a function of temperature and strain rate, as follows

$$\epsilon_f = K \dot{\epsilon}^m \cdot \left[ a_1 \exp \left( - \left| \frac{1}{T} - \frac{1}{T_c} \right|^{1.5} \cdot \frac{Q}{R a_2} \right) + a_3 \right] \quad (1)$$

where,  $Q$  is the thermal activation energy;  $R$  is the universal gas constant,  $8.31 \text{ J} \cdot \text{mol}^{-1} \cdot \text{K}^{-1}$ ;  $T_c$  is the critical temperature; and  $K$ ,  $m$ ,  $a_1$ ,  $a_2$  and  $a_3$  are material constants. It can describe not only the microscopic thermal vibrations of dislocations, but also a characterization of the thermal diffusion of alloying elements. Considering the effect of  $Q$  on  $\epsilon_f$ ,  $Q$  was introduced into the model of the critical fracture strain.

There are seven parameters  $K$ ,  $m$ ,  $a_1$ ,  $a_2$ ,  $a_3$ ,  $Q$  and  $T$  in Eq. (1) that need to be determined.  $T_c$  was obtained by taking an average of all the critical temperature at various strain rates, namely,  $T_c = 1423 \text{ K}$ . The other parameters were determined below.

#### 3.1 Determination of $Q$

According to the literature<sup>[15-17]</sup>, the value of  $Q$  is often determined by using the hyperbolic sine function or exponential function. Comparing the hyperbolic sine function with exponential one, it can be found that there are good linear fitting corrections using an exponential function (see Eq. (2)) at different temperatures and strain rates. So,  $Q$  is given by

$$Q = R \left[ \frac{\partial \ln \sigma}{\partial (1/T)} \right]_{\dot{\epsilon}} \cdot \left[ \frac{\partial \ln \dot{\epsilon}}{\partial \ln \sigma} \right]_{T} \quad (2)$$

where, stress  $\sigma$  is replaced by the peak stress  $\sigma_p$ . It is because that the value of  $\sigma_p$  can reflect the high-temperature characteristics and it is easy to obtain from the tensile tests.

Using Eq. (2), the values of  $n$   $\left( n = \frac{\partial \ln \dot{\epsilon}}{\partial \ln \sigma} \right)_T$  and  $Q$  can be derived from Figs. 4 and 5 as  $n = 6.206$  and  $Q = 352.042 \text{ kJ} \cdot \text{mol}^{-1}$ , respectively.

#### 3.2 Determination of $m$

At constant temperature, Eq. (1) may be rewritten as:

$$m = \frac{\partial \ln \epsilon_f}{\partial \ln \dot{\epsilon}} \quad (3)$$

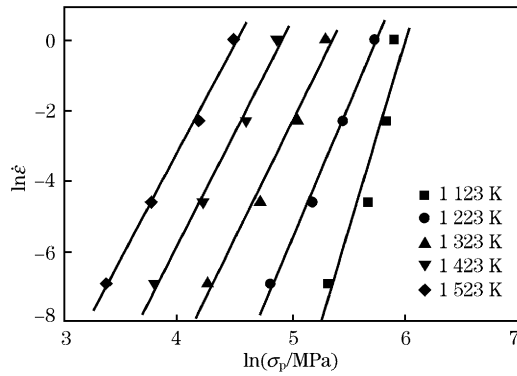


Fig. 4 Correlation of  $\ln \dot{\epsilon}$  and  $\ln \sigma_p$  to determine material constant  $n$

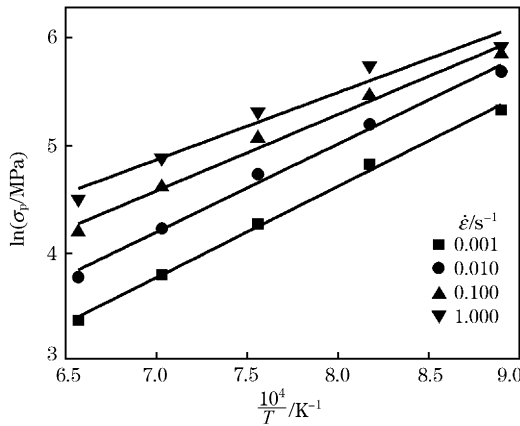


Fig. 5 Correlation of  $\ln \sigma_p$  and  $1/T$  to determine  $Q$

The relationships between  $\ln \epsilon_f$  and  $\ln \dot{\epsilon}$  obtained from the tensile tests are shown in Fig. 6. By using the linear regression technique,  $m = -0.02$  is obtained.

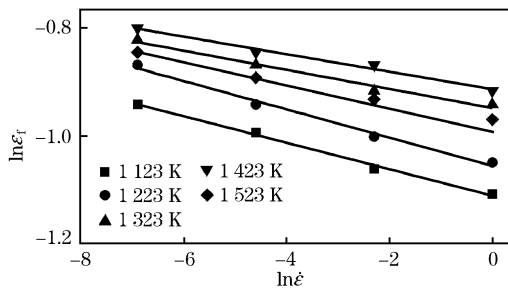


Fig. 6 Correlation of  $\ln \epsilon_f$  and  $\ln \dot{\epsilon}$  to determine  $m$

### 3.3 Determination of $a_1$ , $a_2$ and $a_3$

A least square fit of the results of Fig. 7 yields a power law relation between  $\epsilon_f$  and  $-\left|\frac{1}{T} - \frac{1}{T_c}\right|^{1.5} \frac{Q}{R}$  when  $\dot{\epsilon}$  is constant. The values of  $a_1$ ,  $a_2$  and  $a_3$  can be obtained, namely,  $a_1 = 0.0822$ ,  $a_2 = 0.065$  and  $a_3 = 0.3345$ .

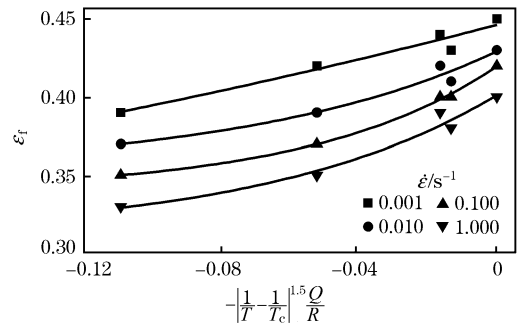


Fig. 7 Relationships between  $\epsilon_f$  and  $-\left|\frac{1}{T} - \frac{1}{T_c}\right|^{1.5} \frac{Q}{R}$  at various strain rates

### 3.4 Determination of $K$

Substituting the parameters  $T_c = 1423$  K,  $m = -0.02$ ,  $a_1 = 0.0822$ ,  $a_2 = 0.065$ ,  $a_3 = 0.3345$  and  $Q = 352.042$  kJ  $\cdot$  mol $^{-1}$  into Eq. (1), the value of  $K$  can be obtained by applying the inverse calculation. And then,  $K$  is calculated as 0.9541. The critical fracture strain model can be expressed as:

$$\epsilon_f = 0.9541 \dot{\epsilon}^{-0.02} \cdot \left[ 0.0822 \cdot \exp\left(-651749 \left| \frac{1}{T} - \frac{1}{1423} \right|^{1.5}\right) + 0.3345 \right] \quad (4)$$

The critical fracture strains at various temperatures and strain rates calculated by Eq. (4) are compared with the experimental results, as shown in Fig. 8. It can be seen that the calculated results are in agreement with experimental ones, and the standard deviation is 0.015.

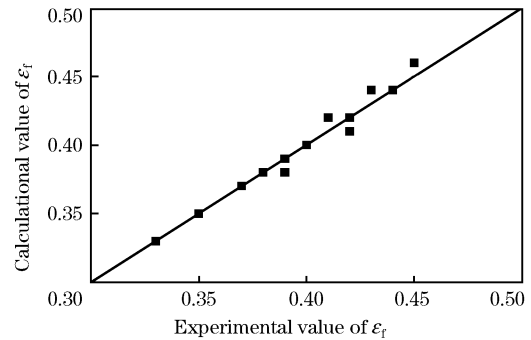


Fig. 8 Comparison of calculated critical fracture strains with experimental results

## 4 Establishment of Ductile Fracture Criterion

A ductile fracture criterion is a quantitative description of the critical fracture occurrence in the forming process. In large plastic deformation process, it is often considered that the ductile damage occurrence results from the nucleation, growth and coalescence of microscopic voids. The micro-voids aggregation

theory is also applied by Oyane<sup>[18]</sup>. And Oyane pointed out that the plastic deformation is concentrated only into narrow regions which interconnect many holes when the volume fraction of voids or the distance between the voids reaches a certain value. Based on these researches, Oyane et al.<sup>[19]</sup> proposed a ductile fracture criterion, and successful predictions of the criterion during bulking forming have been reported by some researchers<sup>[20–22]</sup>. The results show that the Oyane's criterion has high reliability for predicting fracture. As Oyane et al. focused on ductile fracture during the cold forming, this criterion does not consider the effects of temperature and strain rate on ductile fracture. During the hot forming, however, the temperature and strain rate have the effects on ductile fracture and they are the function of the critical fracture strain. Then, the Oyane's criterion can be rewritten as:

$$\int_0^{\bar{\epsilon}_f} \left(1 + \frac{\sigma_m}{B \bar{\sigma}}\right) d\bar{\epsilon} = C_f(\dot{\epsilon}, T) \quad (5)$$

where,  $\sigma_m$  is the average stress;  $\bar{\sigma}$  is the effective stress;  $\bar{\epsilon}_f$  is the equivalent critical fracture strain;  $B$  is a constant that is referred to as the compensation factor of stress; and  $\bar{\epsilon}$  is the equivalent strain. At the right of Eq. (5),  $C_f$  is the criterion of the failure, meaning a critical damage. In the hot forming process, it is variable. The item on the left side of Eq. (5) describes the cumulative damages in the deformation process. In accordance with the definition of the material yield criterion, it is presumed that no matter what the material is in deformed state, the ductile fracture occurs as long as the cumulative damage in the whole deformation process reaches a damage criterion of the critical fracture. In the uniaxial tension test,  $C_f$  can be obtained as:

$$C_f(\dot{\epsilon}, T) \geq \left(1 + \frac{1}{3B}\right) \epsilon_f \quad (6)$$

Taking Eq. (4) into Eq. (6),  $C_f$  is expressed:

$$C_f(\dot{\epsilon}, T) \geq \left(1 + \frac{1}{3B}\right) \cdot 0.9541 \dot{\epsilon}^{-0.02} \cdot [0.0822 \cdot \exp(-651749 \left|\frac{1}{T} - \frac{1}{1423}\right|^{1.5}) + 0.3345] \quad (7)$$

Then, Eq. (7) can be rewritten as:

$$\int_0^{\bar{\epsilon}_f} \left(1 + \frac{\sigma_m}{B \bar{\sigma}}\right) d\bar{\epsilon} \geq \left(1 + \frac{1}{3B}\right) \cdot 0.9541 \dot{\epsilon}^{-0.02} \cdot [0.0822 \cdot \exp(-651749 \left|\frac{1}{T} - \frac{1}{1423}\right|^{1.5}) + 0.3345] \quad (8)$$

However, during the whole deformation process, the temperature and strain rate are not constant. So the deformation process is divided into time steps. In

each time step, temperature and strain rate are taken as constant. The incremental damage and instantaneous  $C_f$  are calculated according to the current temperature and strain rate. The total damage is the integral of the damages in each step. The fracture is regarded to occur by the following equation:

$$\sum_{i=1}^M \left[ \left(1 + \frac{\sigma_{mi}(\dot{\epsilon}_i, T_i)}{B \cdot \bar{\sigma}(\dot{\epsilon}_i, T_i)}\right) \cdot \Delta \epsilon_i \right] / \left(1 + \frac{1}{3B}\right) \cdot 0.9541 \dot{\epsilon}^{-0.02} \cdot [0.0822 \cdot \exp(-651749 \left|\frac{1}{T} - \frac{1}{1423}\right|^{1.5}) + 0.3345] \geq 1 \quad (9)$$

where,  $i$  is the index of time step;  $\Delta \epsilon$  is the instantaneous strain; and  $M$  is the total number of the time steps. The item on the left side of Eq. (9) represents the accumulative damage factor, and the fracture occurs if it is greater than or equal to 1.

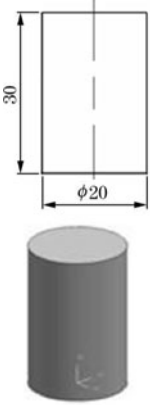
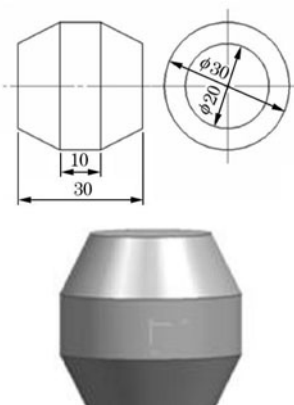
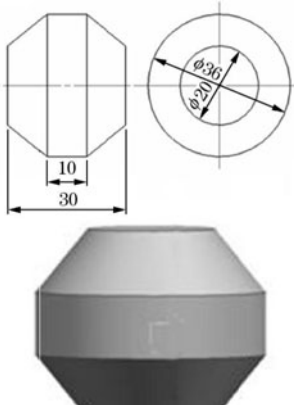
The constant  $B$  is identified by upsetting tests with different shapes in conjunction with FE simulations. One advantage is that the different geometries reflect different stress triaxialities and they have an effect on the damage evolution<sup>[23,24]</sup>. The other advantage is that FE simulation is a widely used and powerful computational tool for quantitatively determining field variables and revealing the deformation behavior of complex deformation processes as demonstrated by Mackerle<sup>[25]</sup>. So, using such method to obtain  $B$  is feasible.

#### 4.1 Experimental procedure and results

The cylindrical upsetting (CUP), tapered upsetting (TUP) and double-cone upsetting (DUP) with the same ratio of height and diameter ( $H/D = 1.5$ ) were conducted to obtain the constant  $B$ . Table 2 shows the detailed experimental design for diverse shapes. The experimental platform was a 100 t hydraulic press. The dry friction condition was used to produce very uneven plastic deformation in order to have a greater rupture tendency<sup>[26]</sup>. The specimens were compressed to different stages in order to capture the cracks initiation moment, which combined with the FE simulations to calibrate the parameter at the temperature of 1473 K and stroking speed of 5.0 mm/s.

The rupture phenomena of the 316LN steel under different deformation scenarios are illustrated in Fig. 9. It can be seen from Fig. 9 that the cracking is initiated at the equatorial free surface of the specimens. The height reduction ratio, which is the ratio of the height reduction to original height of upsetting specimen, is obtained when a surface crack is detected.

**Table 2** 316LN specimens with different geometries and shapes

Cylindrical upsetting ( $H/D=1.5$ , Number=10)	Tapered upsetting ( $H/D=1.5$ , Number=10)	Double-cone upsetting ( $H/D=1.5$ , Number=10)
		

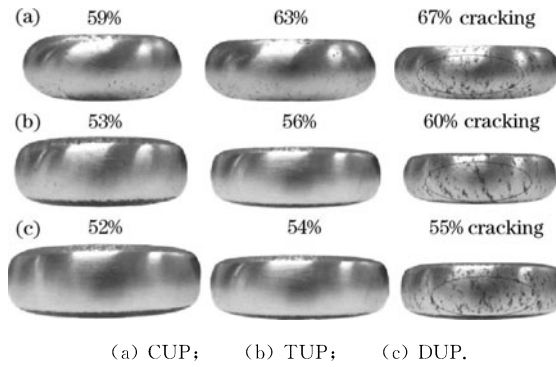


**Fig. 9** Rupture phenomena in the upsetting tests at the temperature of 1473 K and stroking speed of 5.0 mm/s

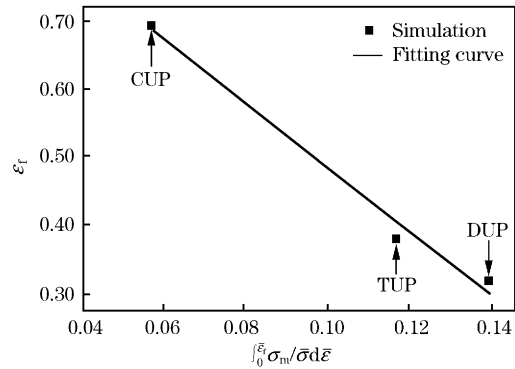


**Fig. 10** Relationship between  $\epsilon_f$  and  $\int_0^{\epsilon_f} \sigma_m/\bar{\sigma} d\bar{\epsilon}$

ted by the visual inspection. It is called the critical height reduction ratio. The critical height reduction ratio of CUP, TUP and DUP tests are 67%, 60% and 55%, respectively, as shown in Fig. 9.

**4.2 FE simulation**

Rigid-plastic FE models were established in the DEFORM-2D platform to simulate the above corresponding upsetting tests. According to the simulated results, the local stress and strain fields were computed accurately when the simulated height reduction ratio was the same as obtained critical height reduction ratio from the experiments (see Fig. 9). Then, the corresponding  $\epsilon_f$  and  $\int_0^{\epsilon_f} \sigma_m/\bar{\sigma} d\bar{\epsilon}$  at the equatorial free surface were obtained. The relationship between  $\int_0^{\epsilon_f} \sigma_m/\bar{\sigma} d\bar{\epsilon}$  and  $\epsilon_f$  for different stress triaxialities was plotted, which is a linear relationship as seen in Fig. 10. Then,  $B$  is easily obtained from the slope of the straight line, viz.,  $B=0.212$ .

Substituting the value of  $B$  into Eq. (9), the ductile criterion of 316LN stainless steel can be obtained as:

$$\sum_{i=1}^M \left[ \left( 1 + \frac{\sigma_{mi}(\dot{\epsilon}_i, T_i)}{0.212 \cdot \bar{\sigma}(\dot{\epsilon}_i, T_i)} \right) \cdot \Delta \epsilon_i \right] / \{ 2.4543 \dot{\epsilon}^{-0.02} \cdot [0.0822 \cdot \exp(-651749 \left| \frac{1}{T} - \frac{1}{1423} \right|^{1.5}) + 0.3345] \} \geq 1 \tag{10}$$

**5 Verification**

In order to validate the proposed ductile fracture criterion, the upsetting tests and the corresponding FE simulations were performed. The upsetting specimens were designed and machined as shown in Fig. 11. Then the specimens were heated to a temperature of 1473 K and held for 20 min. The upsetting tests were conducted by using a 100 t hydraulic press at the stroking speed of 5.3 mm/s when the specimen surface temperature was dropped to 1223 K by the observation of the thermal imager FLIR A615. Each com-

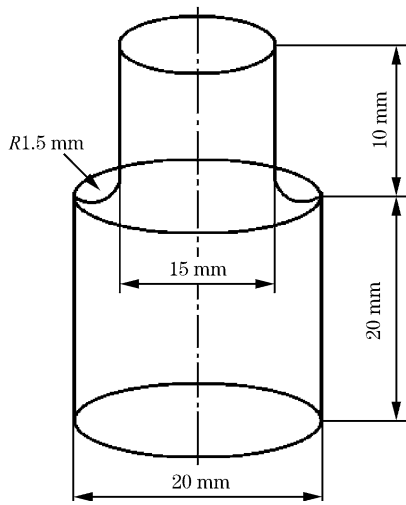


Fig. 11 Schematic diagram of the tensile specimen

pressed specimen was observed by naked eyes after removing the oxide scale on its surface. In order to avoid the influences of internal defects of material and mechanical processing on the occurrence of cracks, the upsetting tests with the same deformation were conducted repeatedly. Fig. 12 shows that the specimens were compressed to different stages until the cracks occurred. The rupture locations under different deformation scenarios were implicated by a small ellipse in Fig. 12. Experimental results show that the cracks usually occur on the free surface when the critical height reduction ratio is up to 56%.

The corresponding FE simulation of upsetting test was carried out under the condition same as actual conditions. The curves of true stress-true strain as shown in Fig. 2 were implanted into the pre-proc-

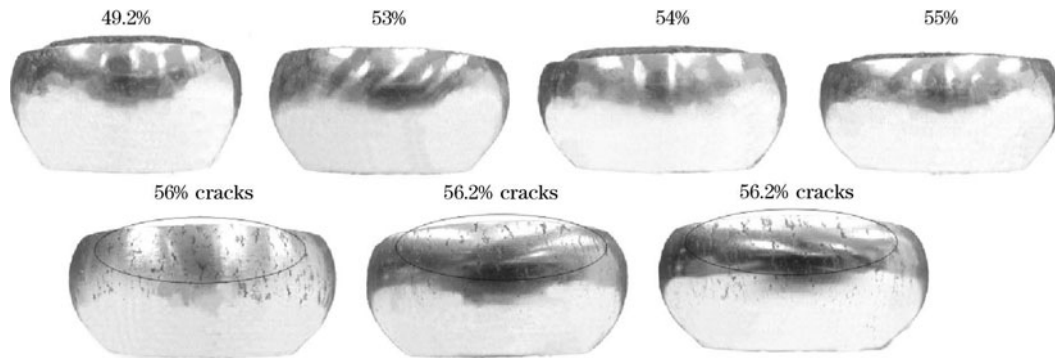
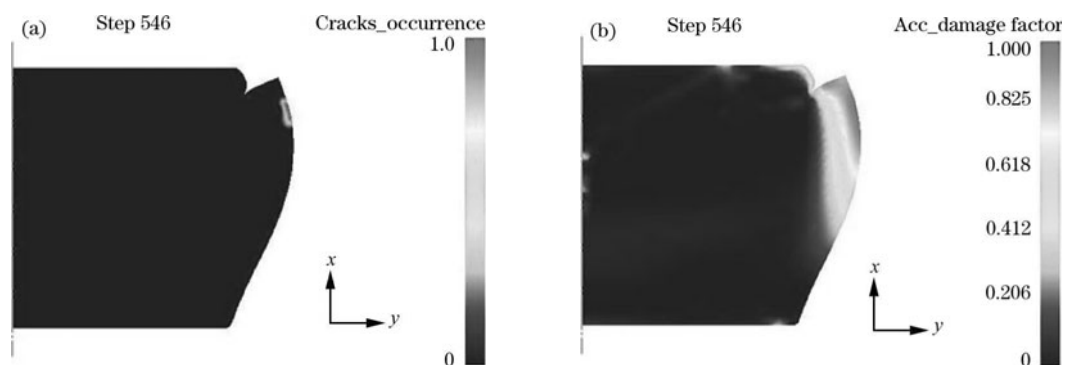


Fig. 12 Upsetting specimens compressed to different stages until the occurrence of cracks and the height reduction ratio being up to 56%

essor. The Young's modulus from the temperature of 923 to 1475 K is in the range of 113.8 to 68 GPa. Poisson's ratio is 0.3. The developed fracture criterion was implemented into the post-processor of DEFORM-2D through user subroutine. Fig. 13 shows

that the cracks occur when the accumulative damage values are equal to 1. At the same time, the height reduction ratio is up to 53%. Comparing Fig. 12 with Fig. 13, there is an agreement between the simulated and experimental results.



(a) Location of the onset of cracks; (b) Accumulative damage values.

Fig. 13 Critical height reduction ratio

## 6 Conclusions

(1) Based on the results of tensile tests, a

model of critical fracture strain as a function of temperature and strain rate was established.

(2) A ductile fracture criterion of 316LN stainless

steel, which considered the effects of the plastic deformation capacity of the material and the stress state, was presented based on Oyane's criterion in conjunction with a model of the critical fracture strain.

(3) The established criterion was integrated with the commercial software DEFORM-2D by user sub-routines to predict the crack initiation and location in the upsetting test. Comparisons between simulated and experimental results indicated that the developed criterion can successfully predict the cracks initiation and location at elevated temperatures.

#### References:

- [1] W. Yang, G. F. Li, C. B. Huang, J. J. Zhou, Z. P. Lu, *Chin. J. Mech. Eng.* 23 (2010) 677-683.
- [2] X. Q. Li, J. J. Zhao, J. C. Xu, X. Liu, *J. Mater. Sci. Technol.* 27 (2011) 1029-1033.
- [3] X. Z. Zhang, Y. S. Zhang, Y. J. Li, J. S. Liu, *Mater. Sci. Eng. A* 559 (2013) 301-306.
- [4] Y. S. Zhang, X. Z. Zhang, X. J. Tian, X. H. Zheng, P. P. Liu, *Forging & Stamping Technology* 36 (2011) No. 6, 1-3.
- [5] X. M. Zhang, W. D. Zeng, Y. Shu, Y. G. Zhou, Y. Q. Zhao, H. Wu, H. Q. Yu, *Trans. Nonferrous Met. Soc. China* 19 (2009) 267-271.
- [6] X. H. Yu, N. Z. Zhai, J. B. Zhai, *Mater. Sci. Technol. China* 17 (2009) 738-740.
- [7] H. Li, M. W. Fu, J. Lu, H. Yang, *Int. J. Plasticity* 27 (2011) 147-180.
- [8] G. Gruben, O. S. Hopperstad, T. Børvik, *Int. J. Mech. Sci.* 62 (2012) 133-146.
- [9] T. Børvik, O. S. Hopperstad, T. Berstad, *European J. Mech. A Solids* 22 (2002) 15-32.
- [10] A. H. Clausen, T. Børvik, O. S. Hopperstad, A. Benallal, *Mater. Sci. Eng. A* 364 (2004) 260-272.
- [11] G. R. Johnson, W. H. Cook, *Eng. Fract. Mech.* 21 (1985) 31-48.
- [12] T. Wierzbicki, Y. B. Bao, Y. W. Lee, Y. L. Bai, *Int. J. Mech. Sci.* 47 (2005) 719-743.
- [13] S. Alexandrov, P. T. Wang, R. E. Roadman, *J. Mater. Process. Technol.* 160 (2005) 257-265.
- [14] J. L. He, Z. S. Cui, F. Chen, Y. H. Xiao, L. Q. Ruan, *Mater. Des.* 52 (2013) 547-555.
- [15] S. S. Bhattacharya, G. V. Satishnarayana, K. A. Padmanabhan, *J. Mater. Sci.* 30 (1995) 5850-5866.
- [16] A. M. Brown, M. F. Ashby, *Scripta Metall.* 14 (1980) 1297-1302.
- [17] C. M. Sellars, W. J. McTegart, *Acta Metall.* 14 (1966) 1136-1138.
- [18] M. Oyane, *Bulletin of the JSME* 15 (1972) 1507-1513.
- [19] M. Oyane, T. Sato, K. Okimoto, S. Shima, *J. Mech. Working Technol.* 4 (1980) 65-81.
- [20] B. P. P. A. Gouveia, J. M. C. Rodrigues, P. A. F. Martins, *Int. J. Mech. Sci.* 38 (1996) 361-372.
- [21] B. P. P. A. Gouveia, J. M. C. Rodrigues, P. A. F. Martins, *J. Mater. Process. Technol.* 101 (2000) 52-63.
- [22] P. McAllen, P. Phelan, *P. I. Mech. Eng. C-J. Mec.* 219 (2005) 237-250.
- [23] N. Bonora, A. Ruggiero, L. Esposito, D. Gentile, *Int. J. Plasticity* 22 (2006) 2015-2047.
- [24] J. H. Giovanola, S. W. Kirkpatrick, *Int. J. Fract.* 92 (1998) 101-117.
- [25] J. Mackerle, *Comp. Mater. Sci.* 31 (2004) 187-219.
- [26] S. Gupta, N. V. Reddy, P. M. Dixit, *J. Mater. Process. Technol.* 141 (2003) 256-265.